$\bar{p}p \to \eta\eta\eta$ from 600 to 1940 MeV/c

D.V. Bugg and B.S. Zou, QMWC, London

1 abstract

Data on $\bar{p}p \to \eta\eta\eta$ are presented. The strongest channel is $f_0(1500)\eta$ from the initial state $^1S_0$. Using in addition data on $\pi^0\pi^0\eta$, we find an upper limit to the branching ratio $BR[f_0(1500) \to \eta\eta]/BR[f_0(1500) \to \pi^0\pi^0] = (0.44 \pm 0.09)$, though possible contamination from $f_2'(1525)$ could reduce this value by up to 15%. A smaller contribution to 3η data from $f_2(1270)\eta$ determines an upper limit to the branching ratio $BR[f_2(1270) \to \eta\eta] = (3.6 \pm 0.4) \times 10^{-3}$, but again possible contamination from $f_0(1370)$ could lower this result by $\sim 30\%$.

2 Introduction

This technical report describes the UK analysis of $\bar{p}p \to 3\eta$ in flight. The data are pretty and seem worth publishing. Nonthetheless, the statistics are low - up to 192 events per momentum - and are such that it is not easy to extract too much physics. In order to focus our minds on the actual content of the data, We have prepared a draft paper intended as a full-length publication, since a letter hardly seems justified. The draft paper contains almost the entirety of the information at our disposal. Therefore the technical report takes the form of this draft paper, plus a few extra Tables as an appendix giving explicit numbers, whose presence in the paper seems unwarranted. For simplicity, the text is exactly as intended for the draft paper and the Appendix which includes extra Tables is self-contained.

The essential results are that branching ratios of $f_2(1270)$ and $f_0(1500)$ to $\eta\eta$ come out in reasonable agreement with earlier GAMS results for $f_2(1270)$ and earlier CBAR results for $f_0(1500)$. That suggests that backgrounds are well under control. It is possible that we shall later get a better estimate of the $f_0(1500)$ branching ratio between $\eta\eta$ and $\pi^0\pi^0$ from data on $3\pi^0$ and $\eta\eta\pi^0$. The statistics on $f_0(1500)$ are larger there by about a factor 5. However, it is already clear that the $f_0(1500)$ sits on top of a broad component in $\pi^0\pi^0$ and it is possible that interferences with the broad component may introduce large uncertainties in the $f_0(1500) \to \pi^0\pi^0$ contribution. That is what happens at rest. Conclusions must await completion of the analysis by Alexei Anisovich of the $3\pi^0$ data. From our completed analysis of $\eta\eta\pi^0$ data, there is no prospect of improving on the result given here for the branching ratio of $f_2(1270)$ to $\eta\eta$; the $f_2(1270)$ signal in $\eta\eta\pi^0$ is simply too small to be clearly visible.

****

As part of a study of $\bar{p}p$ annihilation in flight to neutral final states, we have earlier presented results on $\bar{p}p \to \pi^0\pi^0\eta$ [1], with statistics of typically 70,000 events per momentum. We have at the same time collected statistics of up to 192 events per momentum on $\bar{p}p \to \eta\eta\eta$. Despite the limited statistics, it seems worthwhile to show the data and examine the conclusions which may be drawn from them. To our knowledge, this is the first study of this rare channel.

There is clear evidence in the 3η data for final states $f_0(1500)\eta$ and $f_2(1270)\eta$. Using in addition the data of Ref. [1] on $\pi^0\pi^0\eta$, we are able to estimate the relative branching ratios of $f_2(1270)$ and $f_0(1500)$ to $\eta\eta$ and $\pi^0\pi^0$. However, a difficulty in both cases is the possibility of weak backgrounds, from $f_2'(1525) \to \eta\eta$ and $f_0(1370) \to \eta\eta$, on which we can only set upper bounds.

3 Data Processing

The data were taken at LEAR using the Crystal Barrel detector. Experimental details have been given in Ref. [1], and here we consider only features which involve identification of the 3η final state. In order to isolate this rare channel, tight selection criteria are needed to eliminate backgrounds from other channels. A Monte Carlo study using 20,000 generated events for all competing channels shows that the main sources of potential background are $\eta\eta\pi^0$, $\eta\pi^0\pi^0\pi^0$, $\eta\eta\pi^0\pi^0$, and $\omega\eta\pi^0$ or $\omega\eta\eta$ followed by $\omega \to \pi^0\gamma$. In the last four cases, one or two photons go undetected.

In processing data, we first demand exactly six photon showers, each confined to a block of 3×3 adjacent CsI crystals of the detector. Extra energy deposits produced by Compton scattering out of the primary showers into nearby crystals (so-called 'split-offs') appear in $\sim 50\%$ of events. However, all attempts to recover such events lead to backgrounds higher by typically a factor 3-4. For the present analysis, we therefore reject events containing such additional energy deposits.

A least squares kinematic fit is first required to $\bar{p}p \to 6\gamma$, satisfying energy-momentum balance with confidence level $> 10\%$. Then 7C fits are made to all 3-particle final states involving π^0, η or η'. Events are rejected which fit $3\pi^0$, $\pi^0\pi^0\eta$, $\eta\eta\pi^0$, $\pi^0\pi^0\eta'$ or $\pi^0\eta\eta'$ with confidence level $> 10^{-4}$. As further rejection against the prolific $3\pi^0$ and $\eta\pi^0\pi^0$ channels, events are rejected if they fit $\pi^0\pi^0\gamma\gamma$ or $\pi^0\eta\gamma\gamma$ with confidence level $> 10^{-4}$.

The background levels at 1800 MeV/c from various competing channels are

summarised in Table 1. The principal backgrounds arise from $\omega\eta\eta$, $\omega \to \pi^0\gamma$ after loss of one photon, and from $\eta\eta\pi^0\pi^0$ after two photons are lost. The situation is similar at other momenta and the total surviving background is 2.3% within errors at all momenta. Table 2 shows the reconstruction efficiency ϵ and the number of surviving 3η events after background subtraction. The efficiency is estimated by generating 50,000 Monte Carlo events at momenta from 600 to 1642 MeV/c and 100,000 Monte Carlo events at the highest two momenta; these events are subjected to identical selection procedures to data. They are used for the maximum likelihood fit described below.

4 Features of the Data

Dalitz plots and projections on to $M(\eta\eta)$ are shown at 8 beam momenta from 900 to 1940 MeV/c in Figs. 1 and 2. The $f_0(1500)$ is conspicuous and there are weaker signals due to $f_2(1270)$.

The data have been fitted by the maximum likelihood method. Our strategy is to take magnitudes and phases of all partial waves for $f_2(1270)\eta$ from our earlier analysis of $\pi^0\pi^0\eta$, allowing one free parameter to determine the branching ratio $BR[f_2(1270) \to \eta\eta]/BR[f_2(1270) \to \pi^0\pi^0]$. The $f_0(1500)\eta$ amplitude is fitted freely in magnitude and phase for $L = 0$. Here L is the orbital angular momentum in the production process, $\bar{p}p \to f_0(1500)\eta$. As will be discussed below, there is no evidence for contributions from this channel with $L > 0$, either in the present data or in the $\pi^0\pi^0\eta$ final state. So the final fit uses one complex parameter at each momentum to fit $f_0(1500)\eta$ plus one parameter, common to all momenta, for the $f_2(1270) \to \eta\eta$ branching ratio. Columns 2 and 3 of Table 3 show changes in log likelihood when $f_0(1500)$ or $f_2(1270)$ is removed from the fit. Our definition is such that a change of log likelihood of 0.5 corresponds to a one standard deviation change for one degree of freedom, so the observed changes are quite significant.

Histograms on Figs. 1 and 2 display the results of the fits. The first column of Dalitz plots shows data and the second column shows the fits. Every event is plotted in three $\eta\eta$ combinations. The low statistics cause substantial fluctuations for data and are responsible for some apparent disagreement with the fit, which is much smoother, since the Monte Carlo statistics used in the maximum likelihood fit are over 5000 per momentum. In fact, the χ^2 between data and fit on the Dalitz plot averages 1.1 per point, so there is no systematic discrepancy.

Resonance masses M and widths Γ for $f_2(1270)$ and $f_0(1500)$ are taken from averages of the Particle Data Group (PDG) [2]. The partial wave amplitude

for production of a resonance between particles 1 and 2 then takes the form

$$f = \frac{G}{M^2 - s_{12} - iM\Gamma} B_2(k) B_L(p) Z(\vec{p}, \vec{k}). \quad (1)$$

Here G is a complex coupling constant, s is the mass squared of the $\eta_1\eta_2$ combination, and Z is a Zemach tensor given explicitly in Ref. [1]. The cross section is obtained from the coherent sum of amplitudes for the three $\eta\eta$ combinations. Standard Blatt-Weisskopf centrifugal barrier factors B_L with radius 1.0 fm are used to parametrise the dependence on the centre of mass momentum p with which the resonance is produced and also on its decay momentum k in the resonance rest frame.

The complex coupling constant G assigns a phase to each partial wave. This phase originates from initial state $\bar{p}p$ interaction and from strong interactions involving rescattering in the final state. The approximation we adopt is that the phase is the same for decays $f_2(1270) \to \eta\eta$ and $f_2(1270) \to \pi^0\pi^0$. This is in the spirit of the isobar model, where it is assumed that the final resonant state is reached after any number of intermediate rescatterings and then decays into the $\eta\eta$ and $\pi^0\pi^0$ channels with the same phase. That may be an approximation, since rescattering is possible in $\pi^0\pi^0\eta$ leading to additional final states $a_2(1320)\pi^0$ and $a_0(980)\pi^0$. Results concerning $f_0(1500)\eta$ have little sensitivity to the detailed partial wave decomposition of $f_2(1270)\eta$. This is because correlations between the two channels arise only where bands cross on the Dalitz plots and involve rather few events.

In $\pi^0\pi^0\eta$ data, the contribution from $f_0(1500)\pi$ is small: up to 3.2%, with errors of $\sim 1\%$. It is this uncertainty which will make the largest contribution to the error on the relative branching ratio of $f_0(1500)$ to $\eta\eta$ and $\pi^0\pi^0$. This relative branching ratio comes out to be a factor ~ 40 larger than for $f_2(1270)$, with the result that $f_0(1500)$ makes the larger contribution to 3η data.

For $f_0(1500)\eta$ final states, the angular distributions against centre of mass production angle τ are shown in Figs. 1 and 2. They are isotropic within the limited statistics. A fit with only $L = 0$ is excellent. Adding $L = 1$ gives no significant improvement. Adding $L = 2$ instead gives a marginal improvement which is barely significant statistically. So we adopt the assumption of pure $L = 0$ production.

A point with interesting consequences is that the three $f_0(1500)$ bands cross at the centre of the Dalitz plot near a beam momentum of 1800 MeV/c. The strong constructive interference observed there between the three bands requires that the process goes largely through a single $\bar{p}p$ partial wave. Amplitudes for production with $L = 1$ cancel at the intersection point of the three bands and their sum changes sign about this point. To see this, consider $f_0(1500)$ production from the initial state $^3P_1$. For initial helicity $m = 0$, the

Clebsch-Gordan coefficient for coupling to $\bar{p}p$ is zero. For $m = 1$, the amplitude is proportional to $p \sin\tau \exp(i\phi)$, where τ is the polar angle for production of the resonance and ϕ is the associated azimuthal angle. This amplitude is therefore proportional to $p_X + ip_Y$, where $p_{X,Y}$ are transverse momentum components of the resonance. For the coherent superposition of the three $f_0(1500)\eta$ combinations, the resultant at the intersection of the three bands is zero, by momentum conservation. The same result extends to $L = 3$ for $f_0(1500)\eta$ and production of $f_2'(1525)$ with $L = 1$ and 3, though the amplitude then contains additional factors for the f_2' decay. Fig. 3 shows the predicted Dalitz plot for ${}^3P_1 \to f_0(1500)\eta$ at 1800 MeV/c. This distinctive pattern is absent from the data of Fig. 2. The amplitude analysis confirms that any $L = 1$ or 3 processes producing $f_0(1500)$ or $f_2'(1525)$ at 1642, 1800 and 1940 MeV/c are absent or very weak (summed cross sections $\leq 10\%$ of $L = 0$).

The fourth and fifth columns of Table 3 show changes in log likelihood when either $f_0(1370)\eta$ or $f_2'(1525)\eta$ is added to the fit with $L = 0$. Statistically one expects an improvement of 1 for two extra fitted parameters. The evidence for either $f_0(1300)$ or $f_2'(1525)$ being present is insignificant, but the magnitudes of possible contributions need to be used below in putting limits on branching ratios.

5 Conclusions from the data

Fig. 4 shows the total cross section for 3η (full line), that for $f_0(1500)\eta$, $f_0(1500) \to \eta\eta$ (dotted line) and $f_2(1270)\eta$, $f_2(1270) \to \eta\eta$ (dashed) against $M(\bar{p}p)$. These cross sections have been corrected to allow for all decay modes of the η, i.e. allowing for the 39.25% branching ratio of $\eta \to \gamma\gamma$. The curves on Fig. 4 simply join the points for clarity, and have no physical significance.

There is an important point concerning the $f_0(1500)\eta$ cross section. At individual momenta, the cross section is proportional to the squared modulus of an amplitude containing $f_0(1500)$ contributions in three combinations of η. The interferences enhance the cross section quite considerably where the $f_0(1500)$ bands cross on the Dalitz plot and interfere fully constructively. In order to assess branching ratios of $f_0(1500)\eta$, we also evaluate the cross section with this interference switched off. The result is shown by the chain curve of Fig. 4. For $f_2(1270)$, the corresponding effect is small, since many partial waves contribute and coherence between the three $\eta\eta$ combinations is small.

5.1 $f_0(1500) \to \eta\eta$

The contribution of $f_0(1500)\eta$ to $\pi^0\pi^0\eta$ data is too small to be determined below 1525 MeV. From data at 1525 MeV/c upwards, we deduce a weighted mean

$$\frac{BR[f_0(1500) \to \eta\eta]}{BR[f_0(1500) \to \pi^0\pi^0]} = 0.44 \pm 0.09. \qquad (2)$$

Results are evaluated dropping interferences between the three $f_0(1500)$; these interferences are not a property of the resonance itself, but of the $\bar{p}p$ environment in which it is produced. Branching ratios of the resonance depend only on $|G|^2$ of a single isolated resonance, as discussed by Abele et al. [3].

Earlier results show significant scatter. Values from the PDG are 0.69 ± 0.35 [4] and 0.47 ± 0.21 [5], which agree within the errors with the present value. Abele et al. [3] quote cross sections from which one deduces a value 0.23 ± 0.04, smaller than the present value by ~ 2 standard deviations.

Equn. (2) is, however, subject to possible correction downwards for contamination of 3η data by $f_2'(1525)\eta$. There is no evidence in the $\eta\eta$ mass projection for its presence. Nor does the amplitude analysis find any significant contribution with $L = 0$ or 1. Let α be the decay angle with respect to the beam in the rest frame of the resonance. The decay angular distribution $(3\cos^2\alpha - 1)$ for production from the initial state $^1D_2$ with $L = 0$ is distinctive and the amplitude would interfere with $f_0(1500)\eta$. The $L = 1$ production amplitude likewise gives a distinctive contribution to the Dalitz plot, similar to that of Fig. 3. The mean fitted value of its cross section is 15% of $f_0(1500)\eta$ but some of this is undoubtedly statistical noise in the fit. It would reduce equn. (2) to 0.37 ± 0.08.

5.2 $BR[f_2(1270) \to \eta\eta]$

Fits are made at every beam momentum, varying the magnitude of the $f_2(1270) \to \eta\eta$ branching ratio in steps of 10%. We normalise to the PDG branching ratio $BR[f_2(1270) \to \pi^0\pi^0] = 0.282$. Log likelihood values are summed over all beam momenta and the branching ratio for $f_2(1270)$ is optimised, with the result:

$$BR[f_2(1270) \to \eta\eta] = (3.6 \pm 0.4) \times 10^{-3}, \qquad (3)$$

where the error is purely statistical. This value lies between the GAMS 1983 value [6] of $(5.2 \pm 1.7) \times 10^{-3}$ and their later 1986 value [7] of $(2.8 \pm 0.7) \times 10^{-3}$.

It agrees with the SU(3) prediction [8] $(3.9\pm1.0)\times10^{-3}$, though that prediction is strongly sensitive to the centrifugal barrier.

The value in equn. (3) must again be regarded as an upper limit, since there may be some contamination from $f_0(1370)$. The present data have been examined for a possible contribution from $f_0(1370)\eta$. In view of the fact that $f_0(1500)\eta$ production is consistent with $L = 0$, this is the most likely partial wave for $f_0(1370)\eta$. Estimates of the mass and width of $f_0(1370)$ vary from the PDG value to $M = 1300$ MeV, $\Gamma = 235$ MeV of Abele et al. [3]. Present results are insensitive to these shifts. Two types of test have been applied. Firstly, $f_0(1370)\eta$ production has been added to the fit with $L = 0$ and optimised freely at every momentum. Column 4 of Table 3 shows that there is no significant evidence for its presence; however, the mean contribution is 32% of $f_2(1270)\eta$. Our conclusion is that contamination from $f_0(1370)$ could reduce the ratio given in equn. (3) to $(2.4 \pm 0.4) \times 10^{-3}$. Secondly, the $f_2(1270)\eta$ contribution with $L = 0$ has been replaced by $f_0(1370)\eta$; this gives a considerably worse fit by a difference in log likelihood which is typically ≥ 10.

From earlier analysis of $\bar{p}p \to \eta\eta\pi^0$ and $3\pi^0$ at rest, the ratio $BR[f_0(1370) \to \eta\eta]/BR[f_0(1370) \to \pi^0\pi^0] = 0.056 \pm 0.04$ [6]. Despite the sizable error, there was no doubt of the presence of some $f_0(1370) \to \eta\eta$ signal, considerably higher than that for $f_2(1270)$. From the small $f_0(1370)\eta$ signal in 3η, we therefore deduce that the signal observed in $\pi^0\pi^0\eta$ must be almost entirely $f_2(1270)\eta$ with very little $f_0(1370)\eta$.

5.3 $\sigma \to \eta\eta$

Let us consider the possible contribution to the $\eta\eta$ channel from the broad component of the $J^{PC} = 0^{++}$ amplitude, which is well known to be dominated by $\pi\pi$. We denote this broad component by σ. The present data set a rough upper limit on the branching ratio to $\eta\eta$. This comes about in a very simple way. For $\pi^0\pi^0\eta$ data at 600 MeV/c, there is a significant contribution from the 0^- initial state $\to \eta\sigma$. It is 14%, almost equal to the contribution of $f_2(1270)\eta$ In the present 3η data at 600 MeV/c, there are only 9 events, of which 4 are due to $f_2(1270)\eta$. This implies a low branching ratio of σ to $\eta\eta$. With 90% confidence and allowing for statistical fluctuations, the number of events at 600 MeV/c which might arise from $\sigma \to \eta\eta$ is ≤ 11. This sets an upper limit within the phase space available at 600 MeV/c ($M_\sigma \leq 1414$ MeV) of $BR[\sigma \to \eta\eta]/BR[\sigma \to \pi^0\pi^0] \leq 5\%$. Data at higher beam momenta also show no evidence for a broad component from $\sigma \to \eta\eta$.

6 Conclusions

Despite low statistics, three results emerge from the 3η data.

- The dominant contribution to 3η is from $f_0(1500)\eta$; it is compatible with production purely from the 0^- initial state with $L = 0$. The best estimate of the ratio $BR[f_0(1500) \to \eta\eta]/BR[f_0(1500) \to \pi^0\pi^0]$ is 0.44 ± 0.09, but this could be reduced to 0.37 by weak contamination from $f_2'(1525)$.

- The best estimate for $BR[f_2(1270) \to \eta\eta]$ is $(3.6 \pm 0.4) \times 10^{-3}$, but there is the possibility that contamination by $f_0(1370)$ could reduce this value to 2.4×10^{-3}.

- $BR[\sigma \to \eta\eta]/BR[\sigma \to \pi^0\pi^0] \leq 5\%$ with 90% confidence.

7 Acknowledgement

We wish to thank the technical staff of the LEAR machine group and of all the participating institutions for their invaluable contributions to the success of the experiment. We acknowledge financial support from the British Particle Physics and Astronomy Research Council (PPARC), the German Bundesministerium für Bildung, Wissenschaft, Forschung und Technologie, the Schweizerischer Nationalfonds, the U.S. Department of Energy and the National Science Research Fund Committee of Hungary (contract No. DE-FG03-87ER40323, DE-AC03-76SF00098, DE-FG02-87ER40315 and OTKA T023635). K.M. Crowe and F.-H. Heinsius acknowledge support from the A. von Humboldt Foundation, and N. Djaoshvili from the DAAD. The St. Petersburg group wishes to acknowledge financial support from PPARC and INTAS grant RFBR 95-0267.

References

[1] A. Abele et al, submitted to Nuclear Physics A.

[2] Particle Data Group, Phys. Rev. D54 (1996) 1.

[3] A. Abele et al., Nucl. Phys. A609 (1996) 562.

[4] C. Amsler et al., Phys. Lett. B353 (1995) 571.

[5] C. Amsler et al., Phys. Lett. B355 (1995) 425.

[6] D. Alde et al., Nucl. Phys. B269 (1986) 485.

[7] F. Binon et al., Nu. Cim. 78A (1983) 313.

[8] A. Bramon, R. Casas, J.Casulleras and F. Cornet, Z. Phys. C28 (1985) 573.

Channel	Background (%)
$\eta\eta\pi^0$	0.1
$\eta\pi^0\pi^0\pi^0$	0.1
$\eta\eta\pi^0\pi^0$	1.1
$\omega\eta\eta,\ \omega \to \pi^0\gamma$	0.9
$\omega\eta\pi^0,\ \omega \to \pi^0\gamma$	0.1

Table 1
Background levels from competing channels at 1800 MeV/c.

Momentum (MeV/c)	3η events	$\epsilon(\%)$	$\sigma(3\eta)$ (μb)
600	9	0.130	3.1 ± 1.2
900	68	0.126	3.5 ± 0.5
1050	72	0.126	3.8 ± 0.7
1200	157	0.124	5.8 ± 0.8
1350	103	0.121	6.3 ± 0.8
1525	99	0.117	8.4 ± 1.2
1642	142	0.115	11.1 ± 1.5
1800	192	0.113	11.2 ± 1.3
1940	163	0.112	5.4 ± 1.3

Table 2
Numbers of 3η events after background subtraction, reconstruction efficiency ϵ, and the integrated cross section for 3η (corrected for all η decays) v. beam momentum.

Momentum	$-f_0(1500)\eta$	$-f_2(1270)\eta$	$+f_0(1300)\eta$	$+f_2'(1525)\eta$
900	-27.6	-4.4	1.1	1.2
1050	-25.9	-10.8	1.8	0.9
1200	-44.9	-1.0	1.0	0.1
1350	-56.6	-7.1	2.2	0.8
1525	-15.0	-19.8	0.8	1.7
1642	-21.8	-41.6	4.4	2.0
1800	-95.2	-20.6	0.3	0.5
1942	-50.6	-11.5	4.8	1.1

Table 3
Changes in log likelihood (a) removing $f_0(1500)\eta$ from the fit, (b) removing $f_2(1270)\eta$, (c) adding $f_0(1300)\eta$ and (d) adding $f_2'(1525)\eta$.

8 Appendix

The draft paper above simply quotes a weighted average for the relative branching ratio r_{1500} of $f_0(1500)$ to $\eta\eta$ and $\pi^0\pi^0$. In Table 4 are listed the actual numbers of events for $f_0(1500)$ in 3η, the percentage of $f_0(1500)\eta$ in $\pi^0\pi^0\eta$, the correction factor which allows for self-interferences between $f_0(1500)$ bands, and the resulting value of r_{1500} at each momentum. For those who wish to check the arithmetic in full, it is necessary to use acceptance for 3η given in Table 2 above, that for $\pi^0\pi^0\eta$ and the number of $\pi^0\pi^0\eta$ events in the Technical Report on $\pi^0\pi^0\eta$ in flight.

Momentum (MeV/c)	$N[f_0(1500)]$ in 3η	$f_0(1500)$ in $\pi^0\pi^0\eta$ (%)	Correction factor	$\eta\eta/\pi^0\pi^0$
1350	64	1.1 ± 0.9	0.65	0.56 ± 0.47
1525	66	2.5 ± 0.9	0.70	0.39 ± 0.16
1642	106	3.3 ± 1.0	0.71	0.42 ± 0.14
1800	147	1.44 ± 0.96	0.74	1.23 ± 0.83
1940	114	2.55 ± 0.96	0.75	0.50 ± 0.20

Table 4
Values at individual beam momenta of (i) the number of events fitted to $f_0(1500)$ in 3η data, (ii) the fraction of $f_0(1500)\eta$ in $\pi^0\pi^0\eta$ data, (ii) the correction factor for interferences, (iv) the resulting ratio $BR[f_0(1500) \to \eta\eta]/BR[f_0(1500) \to \pi^0\pi^0]$.

Secondly, Table 5 shows values of log likelihood at individual momenta for five values of $BR[f_2(1270) \to \eta\eta]$; the third column shows the PDG value of

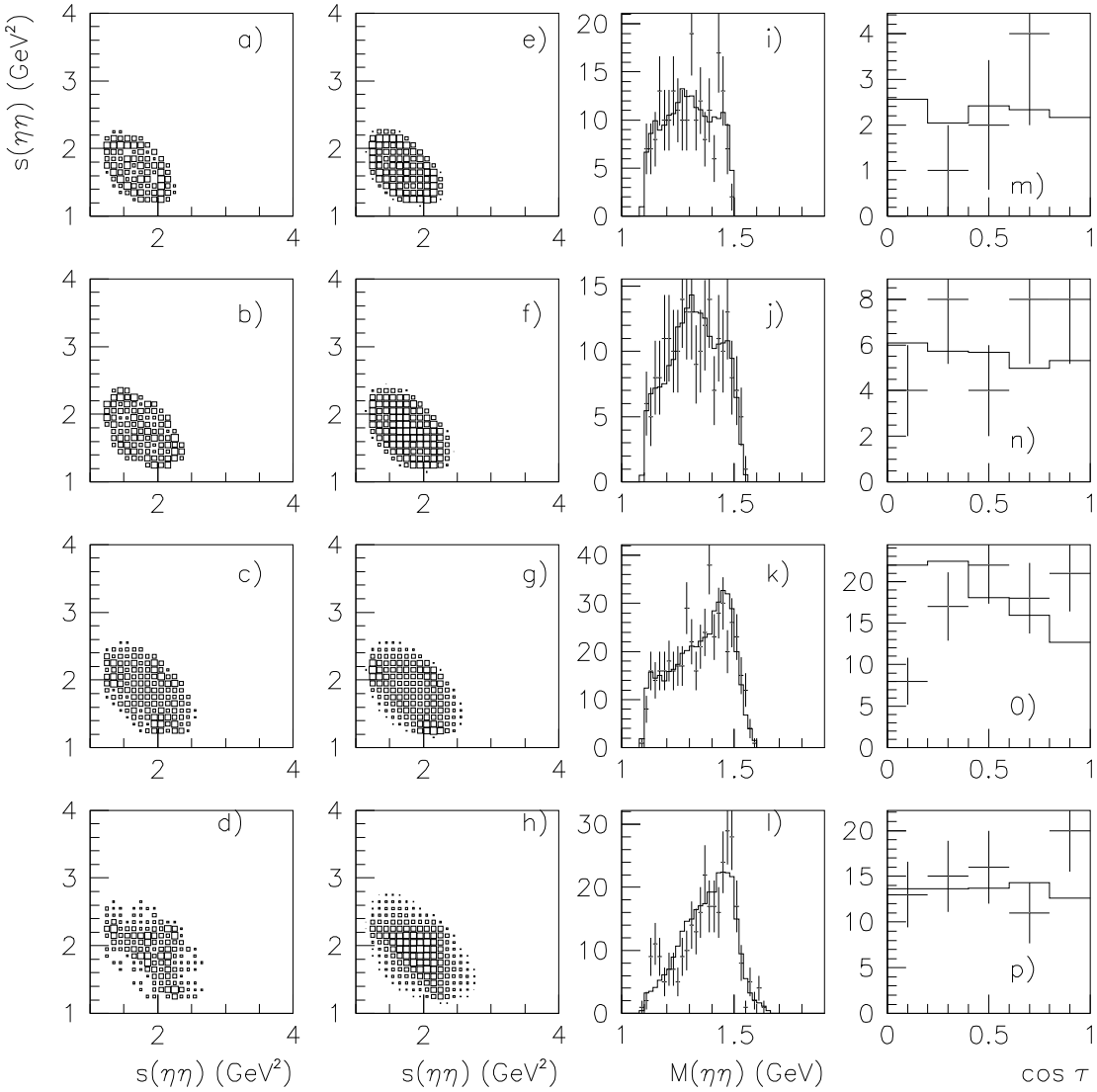

Fig.1. (a)–(d) Dalitz plots of data at beam momenta of 900, 1050, 1200 and 1350 MeV/c, (e)–(h) fitted Dalitz plots, (i)-(l) projections on to $M(\eta\eta)$, (m)–(p) production angular distribution for events in a band 120 MeV wide centred on $f_0(1500)$. Histograms show the fit.

4.5×10^{-3}. The last line of the Table is the sum over momenta and has been used to obtain the best estimate of $BR[f_2(1270) \to \eta\eta$ and its statistical error.

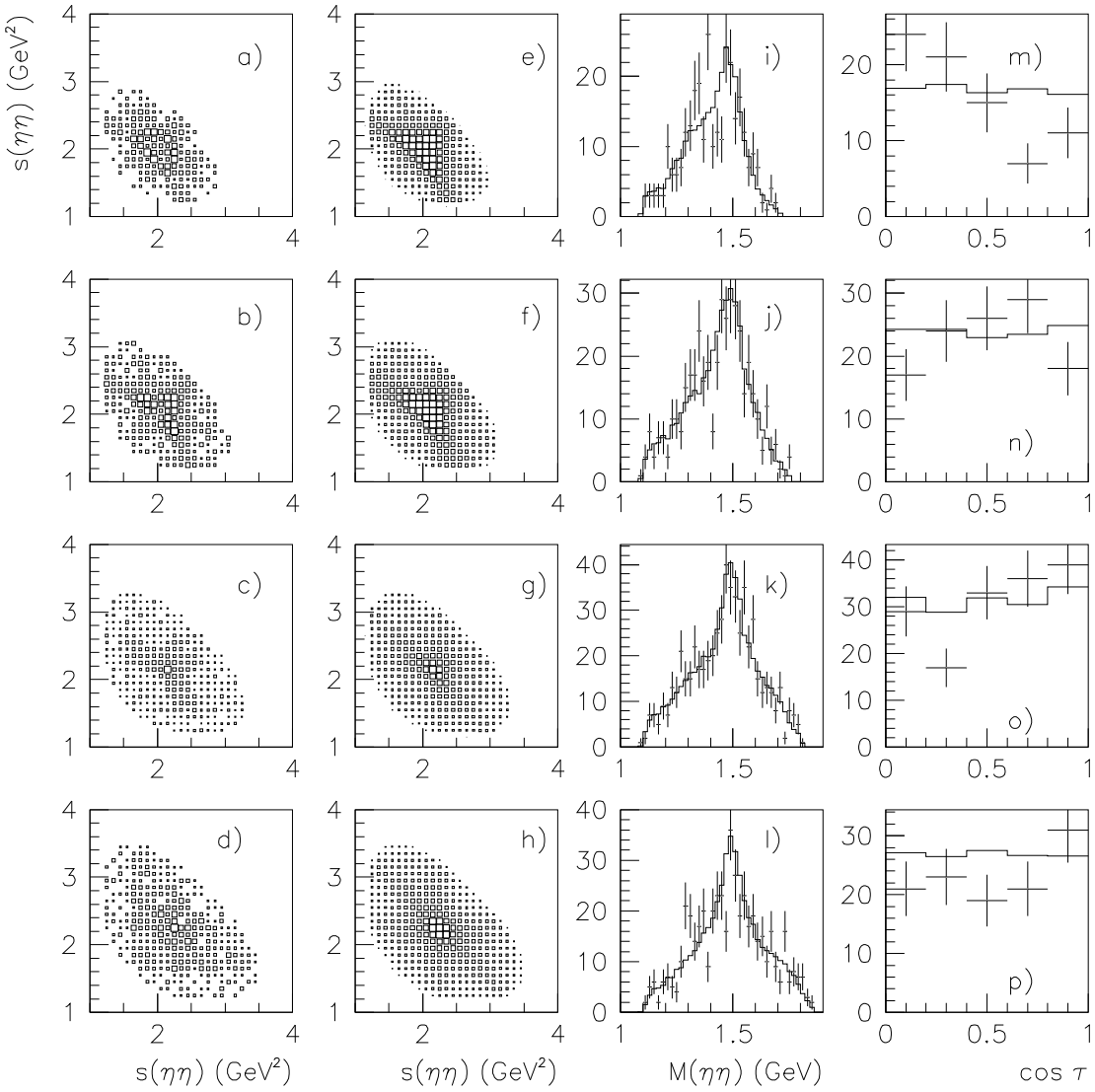

Fig. 2. As Fig. 1 at 1525, 1642, 1800 and 1940 MeV/c.

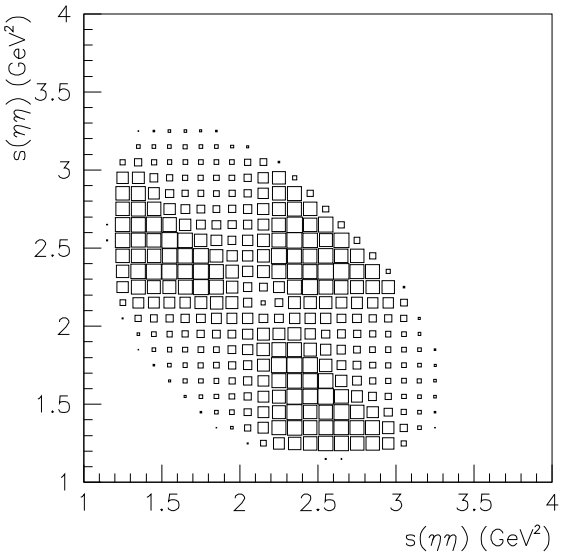

Fig. 3. The Dalitz plot at 1800 MeV/c for ${}^3P_1 \to f_0(1500)\eta$.

Momentum(MeV/c)	5.4×10^{-3}	4.5×10^{-3}	4.05×10^{-3}	3.6×10^{-3}	3.15×10^{-3}
900	-7.91	-8.33	-8.14	-7.71	-7.20
1050	1.83	-2.92	-4.49	-5.51	-6.11
1200	9.04	9.23	9.29	9.28	9.21
1350	-23.00	-26.45	-28.17	-29.87	-31.14
1525	-22.35	-21.61	-21.04	-21.03	-19.38
1642	-32.72	-32.06	-31.47	-30.78	-29.97
1800	-40.18	-40.32	-40.21	-39.91	-39.61
1942	-20.68	-20.20	-19.84	-19.43	-18.95
Total	-135.97	-142.66	-144.07	-144.96	-143.15

Table 5
Values of log likelihood for five values of $BR[f_2(1270) \to \eta\eta$.

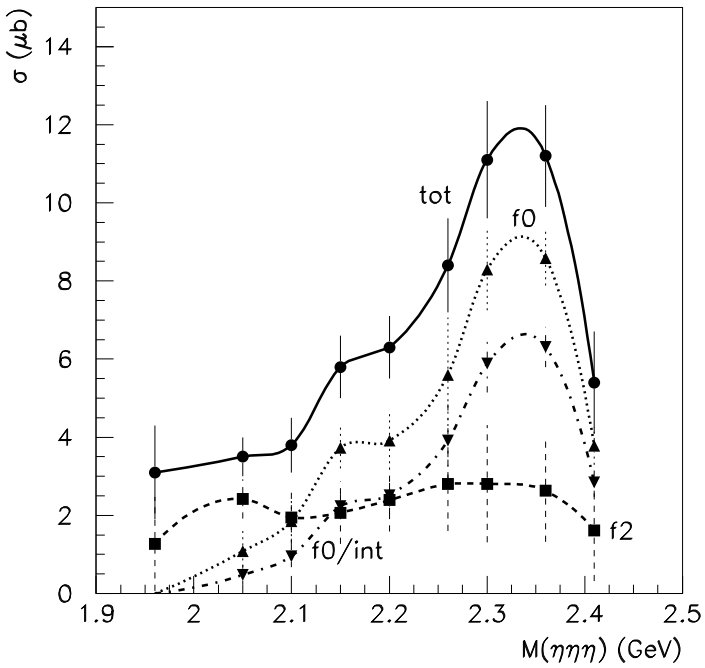

Fig. 4. Cross sections v. $M(\bar{p}p)$ for (a) all events (full line), (b) $f_0(1500)\eta$ (dotted) and $f_2(1270)\eta$ (dashed); the chain curve shows the effect of factoring out from the $f_0(1500)\eta$ cross section the effect of interferences between three $f_0(1500)$ bands on the Dalitz plot, as described in the text.